

Hot Corrosion Behavior of Monel 400 and AISI 304 Dissimilar Weldments Exposed in the Molten Salt Environment Containing $\text{Na}_2\text{SO}_4 + 60\% \text{V}_2\text{O}_5$ at 600 °C

K. Devendranath Ramkumar*, N. Arivazhagan, S. Narayanan, Debidutta Mishra

School of Mechanical & Building Sciences, VIT University, 632014, Vellore, India

Received: February 18, 2014; Revised: July 24, 2014

This research work investigates the use of pulsed current for joining two dissimilar metals Monel 400 and AISI 304 using Pulsed Current Gas Tungsten Arc welding using three different filler metals such as ER309L, ERNiCu-7 and ERNiCrFe-3. Microstructure observations showed the presence of Partially Melted Zone (PMZ) at the heat affected zone (HAZ) of all the weldments. The formation of secondary phases was witnessed at the HAZ of Monel 400 on using ERNiCu-7 filler. Tensile studies corroborated that the bimetallic combinations employing ERNiCu-7 offer better tensile properties as compared to ER309L and ERNiCrFe-3 weldments. Parent metal Monel 400 exhibited better corrosion resistance as compared to other zones of the weldments when exposed in the synthetic molten salt environment containing $\text{Na}_2\text{SO}_4 - 60\% \text{V}_2\text{O}_5$ environment at 600 °C. A detailed structure - property relationship was made using the combined techniques of optical microscopy and SEM. Also the hot corrosion products were revealed using the thermogravimetric plots, XRD and SEM/EDAX analysis.

Keywords: Monel 400, AISI 304 stainless steel, filler metals, mechanical properties, hot corrosion

1. Introduction

Dissimilar metal welding is generally more challenging than that of similar metals, because of the difference in the physical, mechanical and metallurgical properties of the parent metals to be joined¹. Due to the differences in the chemical composition and thermal expansion coefficients, the major problems likely to occur during welding would be improper dilution of weld metals, HAZ liquation cracking, hot cracking and the formation of secondary phases. Bimetallic combinations of Monel 400 and AISI 304 can be used in moderately high temperature and corrosive environments as in the case of oil gasification plants, chemical processing equipments etc. In addition, a combination of moderate oxidation resistance and creep strength extends their application to steam generator tubing and other components operating at temperatures up to 550 °C in conventional fossil-fuel power plants².

Investigations on pulsed current GTA welding on similar metal combinations were studied by different researchers such as in Inconel by Janakiram et al.³, aluminium alloys by Madhusudhan Reddy et al.^{4,5}, Tantalum by Grill⁶. Elemental migration during welding process is one of the major concerns which affect the mechanical and corrosion properties^{7,8}.

Dilution has been a major problem in the dissimilar weldments that have been applied for sheathing the offshore structures of corrosion-poor steels with corrosion resistant Ni-Cu/Cu-Ni alloys. Rudovskii⁹ studied the dilution at the fusion boundary of austenitic stainless steel welded with the filler metal of Monel-400.

Paul et al.¹⁰ investigated the mass transport of the elements like Cr, Ni in Monel 400. A 3D thermo-mechanical

simulation model was developed to predict distributions of temperature and residual stresses during the gas tungsten arc welding (GTAW) process with a heat sink for Monel 400 plates using finite element method¹¹. Weight loss technique during the dissolution of pure Cu, 90/10 and 70/30 Cu-Ni alloys and of Monel 400 in strongly aerated 0.1 M HCl at 25 °C and 60 °C was investigated by Shams El Din et al.¹². The combination of Monel 400 and low carbon steel² was welded by SMAW using ERNiCu-7 and ERNiCrFe-3 filler wires and it was characterized. Such dissimilar weldments are employed in the oil gasification plants. It is to be noted that these plants employ such weldments exposed to corrosive medium of H_2S , SO_2 and SO_3 .

Kim et al.¹³ reported the use of Cr free consumable such as ERNiCu-7 filler for joining austenitic stainless steels. The authors claimed that better corrosion properties could be accrued on using the Monel filler. The pitting corrosion resistance was observed to be good on using ERNiCu-7 filler. Liang et al.¹⁴ addressed the use of Ni-Cu-Pd metal can be a potential replacement for the conventional SS308L filler metal for joining SS304.

Due to depletion of high-grade fuels and for economic reasons use of residual fuel oil in these energy generation systems is well known. Residual fuel oil contains sodium, vanadium and sulphur as impurities. Sodium and sulphur form Na_2SO_4 (melting point 884 °C) by reactions in the combustion system. Whereas during combustion of the fuel, vanadium reacts with oxygen to form an oxide V_2O_5 (melting point 670 °C). According to Otero et al.¹⁵, Na_2SO_4 -60% V_2O_5 deposit was detected on a number of components in actual service which were operated at high temperature and were in contact with high-temperature gases from combustion of dirty fuels, containing certain amounts of impurities, i.e. Na,

*e-mail: deva@vit.ac.in

V, S etc. The presence of sulphur and its oxidised compounds were reported to favour the formation of isolated lobes with radial morphology having great permeability to facilitate the access of oxygen which further leads to reduction in the protecting behavior of scale. The presence of vanadium and its oxidised products was observed to generate compounds with aciculate morphology, identified to look like alkaline vanadate complexes.

Devendranath et al.¹⁶ investigated the performance of GTA weldments of Monel 400 and stainless steel in the molten salt environment containing $K_2SO_4 + NaCl$ at 600 °C. As evident from the open literature, the dissimilar combinations of Monel 400 and stainless steel have typical applications in petrochemical, chemical and nuclear power plants where the hot corrosion environments are prevailing which could deteriorate the properties.

In the present investigation, an attempt has been made to study the dissimilar welds of Monel 400 and AISI 304 stainless steel obtained by pulsed current gas tungsten arc welding process. The filler wires employed in this study are ER309L, ERNiCu-7 and ERNiCrFe-3. The mechanical and metallurgical properties of these dissimilar weldments are studied. Further a detailed analysis has been made to assess the hot corrosion behavior by exposing the coupons of the weldments in the molten salt environment containing $Na_2SO_4 + 60\% V_2O_5$ environment.

2. Experimental Procedure

2.1. Candidate metals and welding procedure

The chemical composition of the base and filler metals employed in this study is given in Table 1. Before welding, the as-received base plates were cut using wire-cut Electrical Discharge Machining (EDM) process and the dimensions of the samples were 100 mm × 50 mm × 6 mm. The process parameters were established based on the bead on weld studies and also by trial runs. The weld process parameters employed for PCGTA welding of Monel 400 and AISI 304 stainless steel is represented in Table 2. The filler wires

employed in this study were ER309L, ERNiCu-7 and ERNiCrFe-3.

PCGTA welding was carried out on these dissimilar metals using a special welding jig (rigid fixture) with a copper back plate so as to hold the parts in alignment and to ensure for accurate grip without bending. Standard butt joint configuration (single V-groove having a root gap of 2 mm, size land of 1 mm and included angle of 70°) was chosen for the current study. The weldments obtained by PCGTA welding technique employing different filler wires were assessed for their metallurgical, mechanical properties and hot corrosion behavior and are outlined in the subsequent chapters.

2.2. Metallurgical and mechanical characterization of weldments

After welding, the PCGTA weldments were characterized using X-ray radiography NDT technique to determine the weld defects. Ensuuing to the NDT results, the welded samples were sliced into coupons of various dimensions to conduct metallurgical, mechanical and hot corrosion tests. Dissimilar weld combinations of AISI 304 and Monel 400 were examined for microstructure at various zones of the weldment using optical microscope. Metallographic examination has been carried out on the region named as 'composite region' whose dimensions are 30 mm × 10 mm × 6mm which covers all the zones (Parent metals - Heat Affected Zones (HAZs) - Weld Zone) of the weldments. The composite region of the weldments were polished as per the standard metallographic procedures including polishing with emery sheets of SiC with grit size varying from 220 to 1000 and followed by disc polishing using alumina and distilled water to obtain a mirror finish of 1 μ on the weldments. Microstructures of parent metal and HAZ of Monel 400 are characterized using Marble's reagent and for parent metal and HAZ of AISI 304, electrolytic etching (10% Oxalic Acid; 6 V DC supply; current density of 1 A/cm²) was used. The weld regions are examined using Marble's reagent for ERNiCu-7, ERNiCrFe-3 weldments and electrolytic etching for ER309L weldments. Further the weldments were characterized for the mechanical properties.

Table 1. Chemical composition of base and filler metals.

Base / Filler Metal	Composition, Wt%									
	Ni	Cu	C	Si	Mn	Fe	S	P	Cr	Others
Monel 400	65.38	Bal	0.10	0.40	1.07	2.11	Nil	Nil	Nil	---
AISI 304	8.13	Nil	0.045	0.39	1.64	Bal	0.006	0.022	18.01	---
ER309L	12.6	---	0.035	0.53	1.58	61.76	0.021	0.024	Bal	Nil
ERNiCu-7	67.6	Bal	0.03	0.9	3.2	0.95	0.006	0.009	---	0.05 (Al) 0.65 (Ti)
ERNiCrFe-3	61.2	0.5	0.05	0.8	5.5	10.5	0.015	0.03	Bal	0.8 (Al) 1.5 (Nb) 0.68 (Mo)

Table 2. PCGTA Weld process parameters for Monel 400 and AISI 304.

Filler wire	Peak Current (I _p) Amps	Base Current (I _b) Amps	Frequency (Hz)	No. of Passes	Argon Gas Pressure (psi)	Filler wire dia. (mm)
ERNiCu-7	215	125	8	6	10-15	2.5
ER309L	215	125	8	6	10-15	2.4
ERNiCrFe-3	215	125	8	6	10-15	2.4

Micro-hardness studies were carried out on the composite region of the dissimilar weldments of Monel 400 and AISI 304 across the entire width of the weldments by keeping weld as center using Vicker's Micro-hardness tester. A standard load of 500 gf is applied for a dwell period of 10 s and the measurements were carried out at regular intervals of 0.25 mm. Further to evaluate the weldments for tensile properties, the samples are typically dimensioned as per ASTM E-8 standards and the tensile tests were performed using the Instron Universal testing machine. Three trials on each weldment were conducted to check the reproducibility of the results. The crosshead velocity of the instrument was maintained constant as 2 mm/min. to exhibit the required strain rate for the tensile studies. The fractured samples were characterized to understand the mode of fracture by SEM analysis.

2.3. Cyclic hot corrosion test

To assess the performance of the weldments in the real time environments, the various zones of the welded coupons were subjected to hot corrosion studies. The coupons used for corrosion studies were mirror polished down to 1 μ before the corrosion run. Cyclic hot corrosion studies were performed on different zones of the weldments by exposing in the molten salt environment of Na₂SO₄ + V₂O₅ (60%) mixture at 600 °C. Hot corrosion studies were performed on different zones of dissimilar weldments of Monel 400 and AISI 304 each measuring 10 mm × 10 mm × 6 mm; also on the composite region measuring 30 × 10 × 6 mm to estimate the corrosion behavior for 50 cycles (each cycle consists of 1 h heating followed by 20 min of cooling to room temperature) at 600 °C.

A coating of uniform thickness with 3–5 mg/cm² of Na₂SO₄ + V₂O₅ (60%) was applied using a fine camel hair-brush on the samples. The salt coated samples were first heated and dried at 200 °C in the oven. Each cycle consists of 1 h heating followed by 20 min of cooling to room temperatures. The weight changes have been measured for all regions for each cycle using electronic weighing balance with a sensitivity of 1 mg. The weight gain or loss of the spalled scale was also included at the time of measurement to determine the rate of corrosion. The corroded samples

of various regions were characterized for XRD and SEM/EDAX analysis.

3. Results

3.1. Macro and microstructure of the weldments

It is evident from the photographs and the macrostructure examination shown in Figures 1 and 2 that PCGTA welding employing aforementioned filler metals has shown good fusion of candidate metals employed in the study. NDT results also confirmed that there were no observable macro/micro-scale deficiencies in all the weldments. Microstructure examination on the dissimilar weldments (Figure 3) clearly witnessed the formation of partially melted zone on the HAZ of Monel 400 side on employing ER309L (Figure 3a) and ERNiCu-7 (Figure 3d) filler metals. However the width of this PMZ is minimized as compared to the GTA weldments which were reported by the authors in their earlier work. Liquation cracks were being observed at the HAZ of Monel 400 on employing ER309L. Segregation effects were not being observed on the HAZ of AISI 304 for the ER309L and ERNiCrFe-3 weldments. Grain refinement was observed at the HAZ of both Monel 400 as well as AISI 304 in all the cases.

3.2. Mechanical characterization of the weldments

It is observed from the hardness profile shown in Figure 4 that the average hardness of the weld regions of ERNiCrFe-3 and ER309L weldments is found to be greater as compared to ERNiCu-7 weldments. The hardness trend of ERNiCu-7 weldments showed steady values and almost same in the parent, HAZ and in the weld regions of Monel 400.

From the tensile studies, it is inferred that the weldments employing ERNiCu-7 and ERNiCrFe-3 fillers had shown severe plastic deformation before the fracture whereas no significant plastic deformation was observed in the ER309L weldments. Tensile fracture occurred at the parent metal of AISI 304 for the ERNiCu-7 and ERNiCrFe-3 weldments whereas the fracture was witnessed at the weld zone in case of ER309L weldments (Figure 5). The

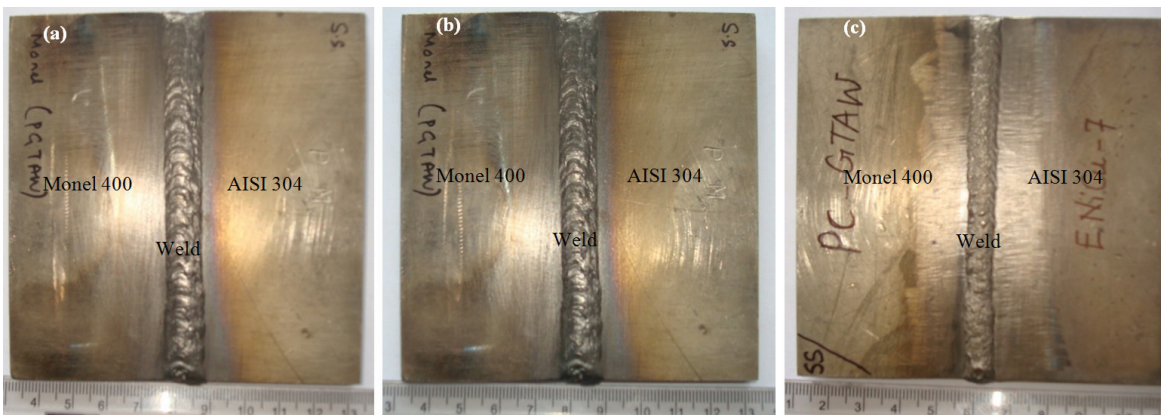


Figure 1. Dissimilar welds of Monel 400 and AISI 304 using (a) ER309L (b) ERNiCu-7 (c) ERNiCrFe-3 by PCGTAW process.

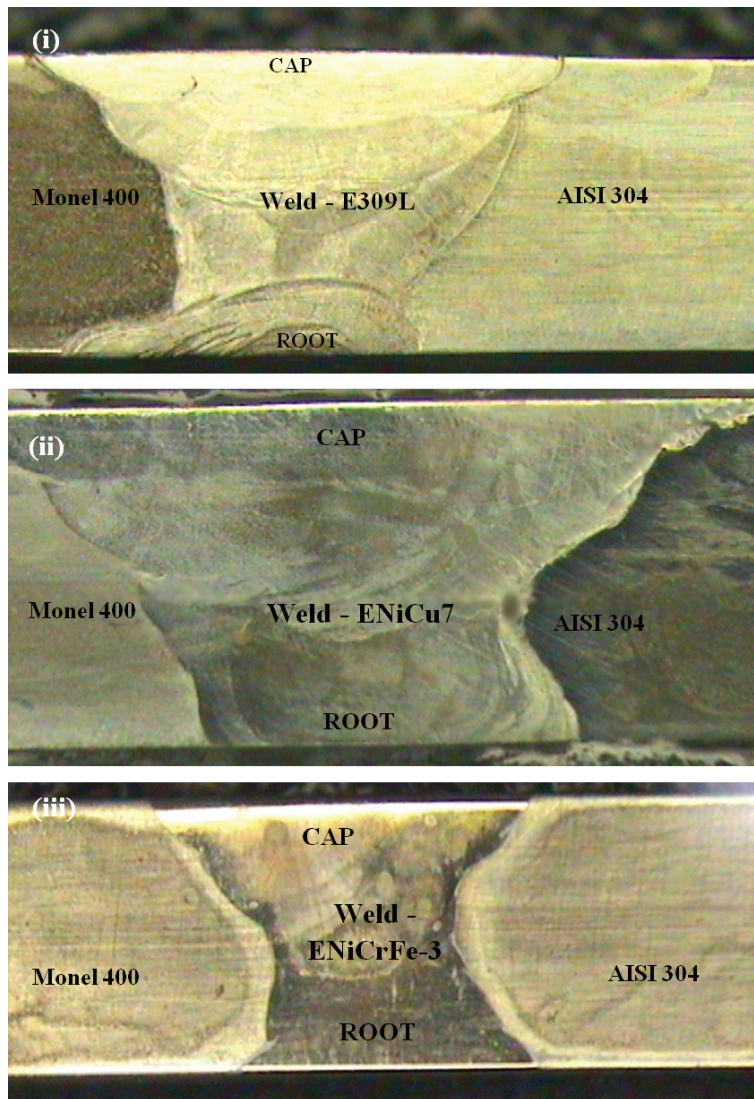


Figure 2. Macro-photographs of the PCGTA welds of dissimilar Monel 400 and AISI 304 using (i) ER309L (ii) ERNiCu-7 and (iii) ERNiCrFe-3.

average tensile strength of ERNiCu-7 and ERNiCrFe-3 weldments was found to be greater as compared to ER309L weldments. Further to find the mode of fracture, SEM analysis was carried out on the fractured samples. SEM fractographs revealed the presence of dimples and microvoids coalescence in the fibrous network of the fractured zones for ERNiCu-7 and ERNiCrFe-3 weldments whereas radiating tearing ridges with less voids were observed on the fractographs of the ER309L weldments shown in Figure 6. The cumulative room temperature tensile properties are listed in Table 3.

3.3. Hot corrosion

3.3.1. Visual examination

During hot corrosion of various zones of PCGTA weldments subjected to $\text{Na}_2\text{SO}_4 + 60\% \text{V}_2\text{O}_5$ environment, the weight and color changes in the samples are discussed.

In case of ER309L weldments, pale golden yellowish spots are observed in the HAZ of AISI 304 during the initial cycles. The weld region has tarnished to brown color with golden yellowish patches at the end of 5th cycle. The color of HAZ of Monel 400 of ER309L weldment has turned to slight greyish appearance at the end of 5th cycle. However more spallation is observed in the weld zone at every cycle. At the end of 50th cycle, the HAZ side of Monel 400 has attained black color with white patches; weld region has become brownish in color with golden orange patches; the color of HAZ side of AISI 304 has become black with few golden yellow spots (Figure 7).

In case of ERNiCu-7 weldments, a rough brown scale is formed on the HAZ of AISI 304; some red spots are formed along with brown scale in the HAZ of Monel 400 and a rough brown scale with white spots are appearing on the weld region. These scales continue to become thicker for every cycle. At the end of 50th cycle, the weld region has tarnished to dark brown

Table 3. Room temperature mechanical properties.

Welding	Filler Wire	Maximum Hardness at weld (HV)	Ultimate Tensile strength (Mpa)	% of Elongation	Fracture Zone -Remarks
PCGTAW	ER309L	260	225	10	Weld region
	ERNiCu-7	206	551	27	Base metal of AISI 304
	ERNiCrFe-3	365	537	27	Base metal of AISI 304

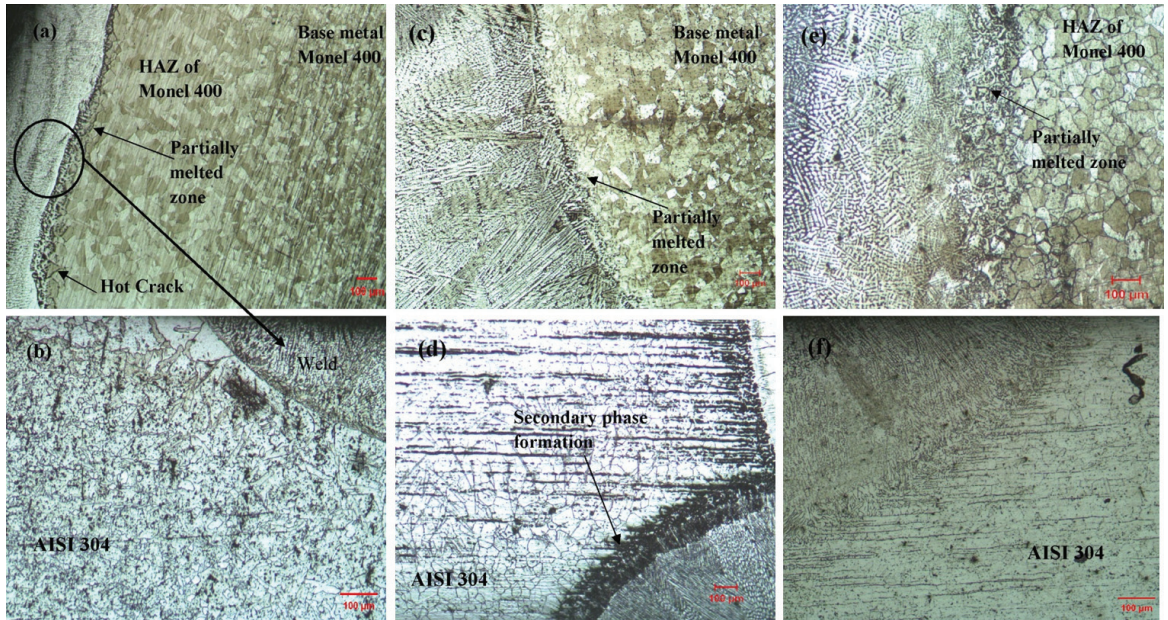


Figure 3. Microstructures showing the PCGTAW welds of dissimilar Monel 400 and AISI 304 using E309 L filler wire (a, b); ERNiCu-7 filler wire (c, d); ERNiCrFe-3 filler wire (e, f).

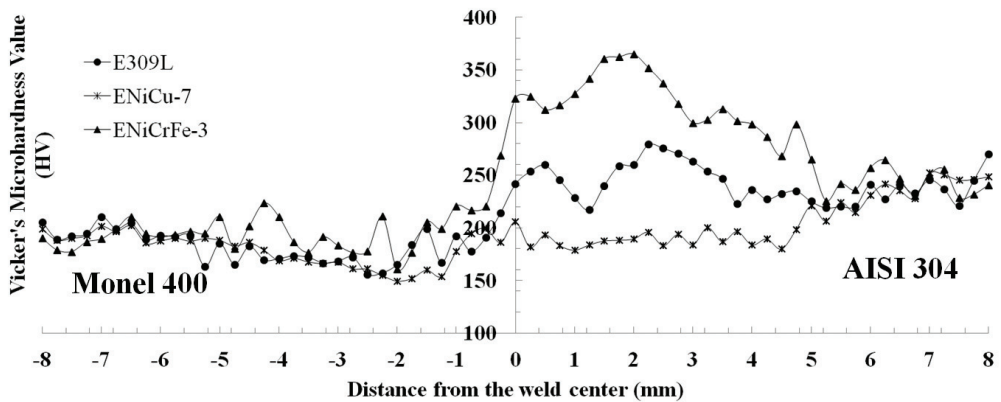


Figure 4. Hardness profile of the PCGTAW dissimilar combinations of Monel 400 and AISI 304.

color with white spots across the entire sample; the HAZ of Monel 400 has become brown colored. On HAZ of AISI 304, the appearance has changed to dark brown color with few faded golden yellowish patches of the dried salt (Figure 7).

On the other hand, for ERNiCrFe-3 weldment, the appearance of HAZ of AISI 304 has changed from slight grey color to dark brown color during the course of corrosion. The scale formed on this region has a rough reddish layer with few white spots. The color of the weld region is changed to dark brown color from 5th cycle and the scale continued to become thicker. At the end of 50th cycle,

the HAZ of Monel 400 has attained dark brown color with greenish patches; weld region tarnished to brown color with greyish green patches surrounding it; the HAZ of AISI 304 has turned to black color with white patches (Figure 7).

3.3.2. Thermogravimetric analysis

Thermogravimetric plots indicate the cumulative weight gain (mg/cm²) as a function of time (number of cycles) of PCGTAW welded dissimilar Monel 400 and AISI 304 subjected to Na₂SO₄ + V₂O₅ (60%) up to 50 cycles (Figures 8a to 8c). The spalled scale is also included at the time of

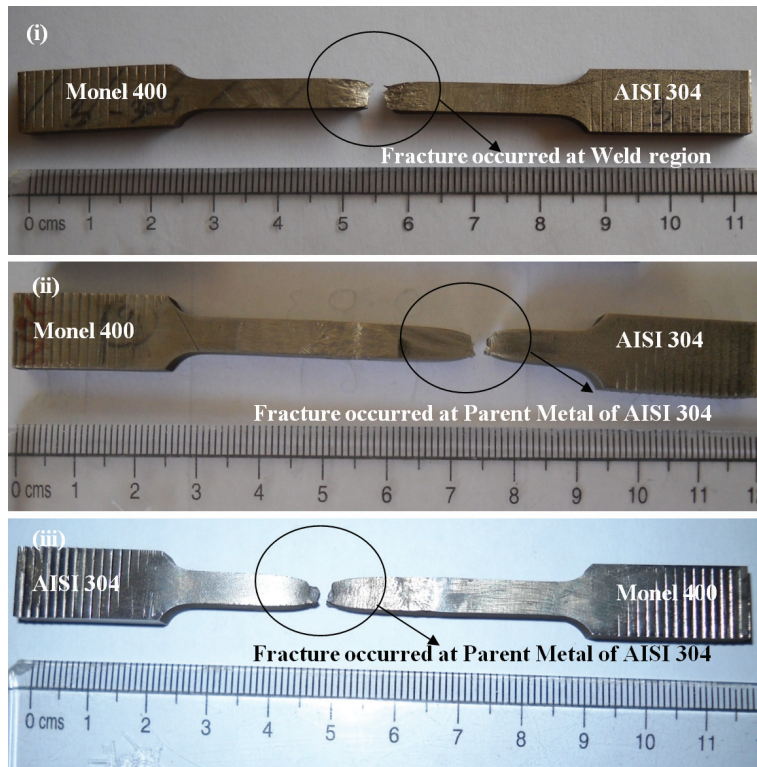


Figure 5. Fractured tensile samples of PCGTA welds of Monel 400 and AISI 304 using (i) ER309L (ii) ERNiCu-7 and (iii) ERNiCrFe-3 filler wires.

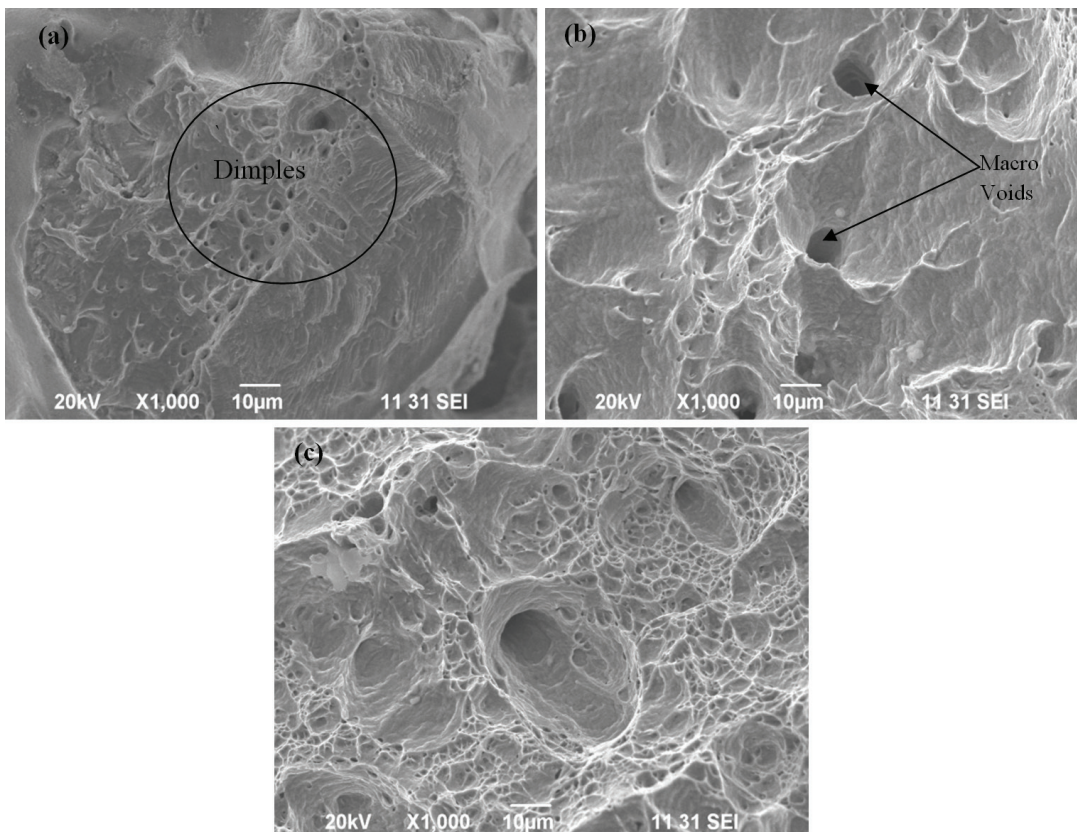


Figure 6. SEM fractographs of the PCGTA welds of dissimilar Monel 400 and AISI 304 using (a) ER309L (b) ERNiCu-7 (c) ERNiCrFe-3.

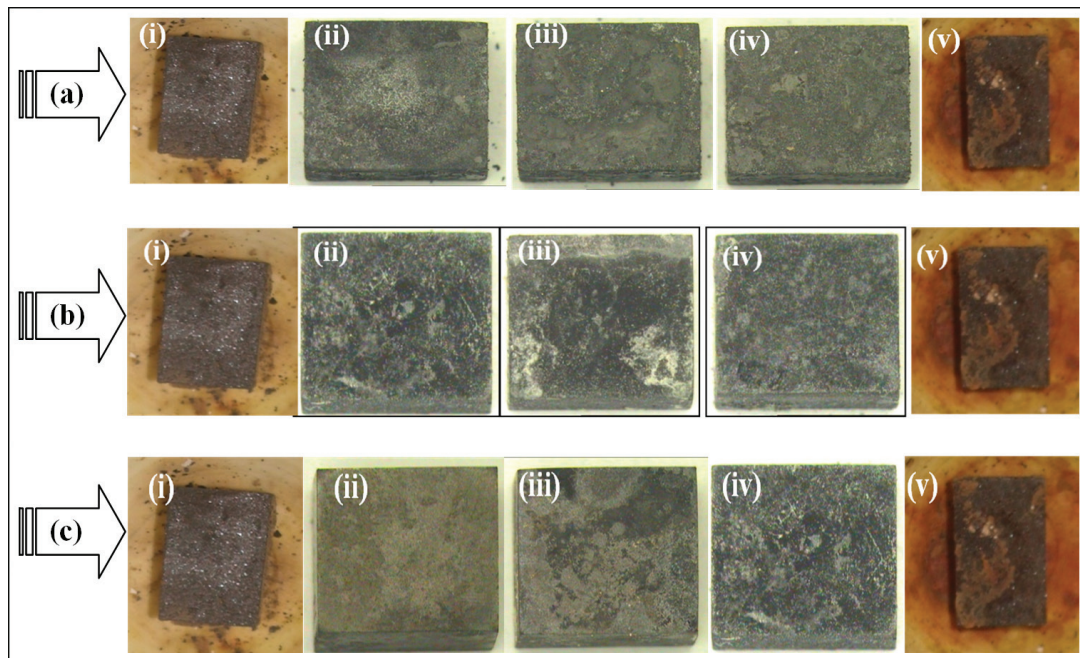


Figure 7. Macrographs of the hot corroded samples of GTA weldments employing (a) ER309L (b) ERNiCu-7 and (c) ERNiCrFe-3 filler wires representing the zones (i) Parent metal - AISI 304 (ii) HAZ - AISI 304 (iii) Weld (iv) HAZ - Monel 400 (v) Parent metal - Monel 400 subjected to the molten salt environment of Na₂SO₄ + 60% V₂O₅ at 600 °C.

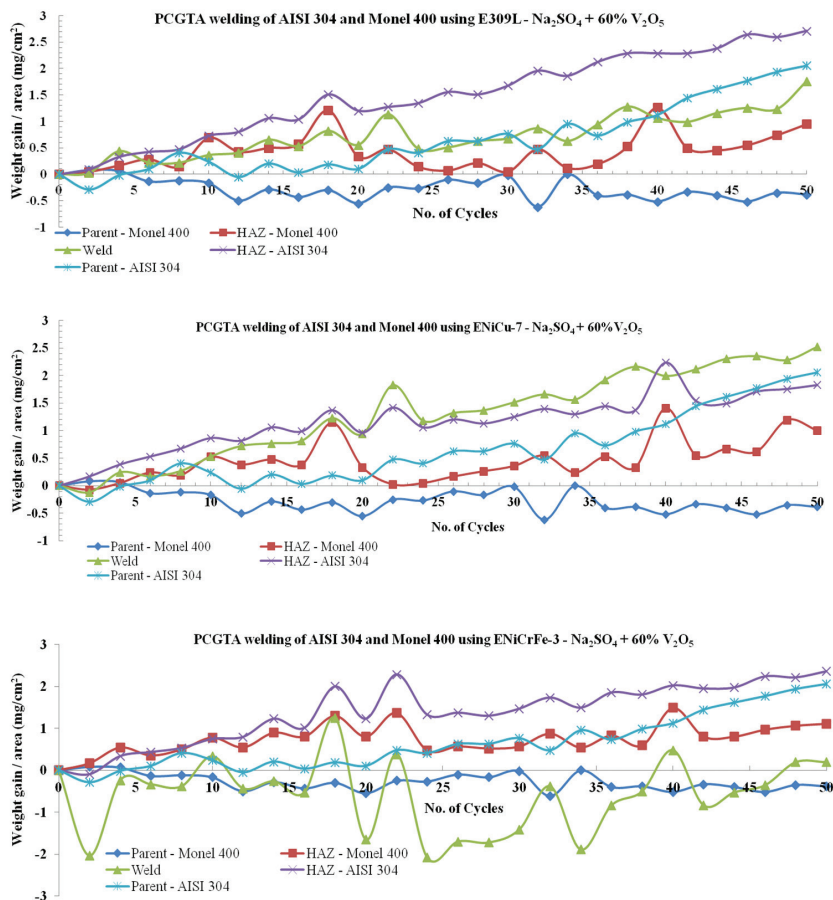


Figure 8. Thermogravimetric data of PCGTA welded dissimilar Monel 400 and AISI 304 subjected to the molten salt environment of Na₂SO₄ + 60% V₂O₅ at 600 °C (a) ER309L (b) ERNiCu-7 and (iii) ERNiCrFe-3 weldments.

measuring the weight changes. From the thermogravimetric analysis, it is clear that HAZ of AISI 304 has maximum weight gain for ER309L and ERNiCrFe-3 filler wires; whereas the weld region has maximum weight gain in ERNiCu-7 filler wire. The parent metal of Monel 400 has shown better corrosion resistance amongst other zones of the weldments. Furthermore, it is observed that the weight changes are fluctuating and hence do not obey the parabolic rate law.

3.3.3. XRD analysis

After corrosion, the composite regions of the various weldments are examined for XRD analysis and are shown in (Figure 9). XRD analysis of ER309L weldment reveals that NiO and, Cu₂O form the predominant phase and also considerable amounts of Cr₂O₃ and FeO were present. In case of ERNiCu-7, the major peak intensities formed on the region include NiO, Cu₂O, Ni₂CuO₃ and lower intensities of FeO and Cr₂O₃. On the other hand, the major

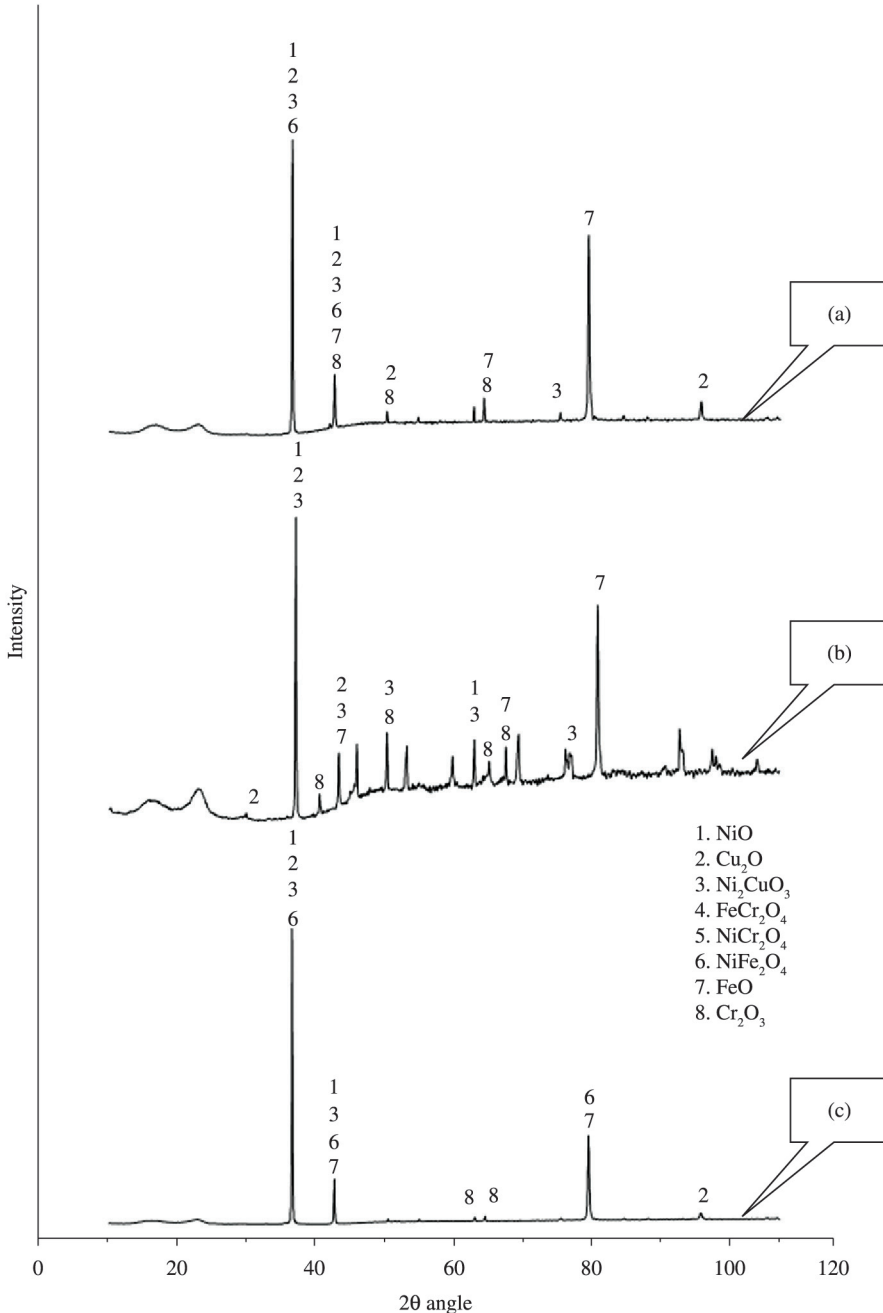


Figure 9. XRD analysis of hot corroded PCGTA welded dissimilar Monel 400 and AISI 304 (Composite Region) employing (a) ER309L (b) ERNiCu-7 and (c) ERNiCrFe-3 subjected to the molten salt environment of Na₂SO₄ + 60% V₂O₅ at 600 °C.

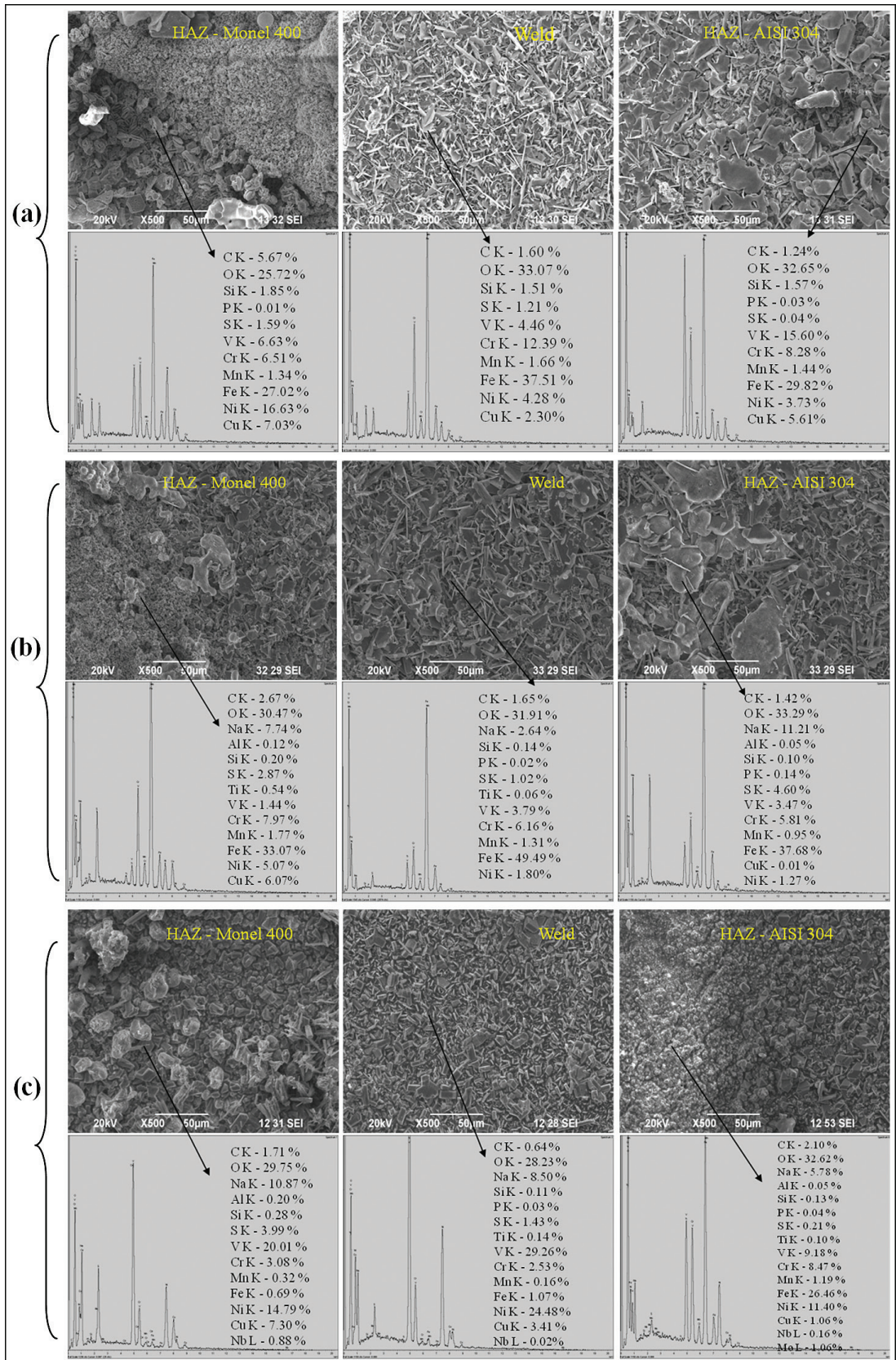


Figure 10. SEM/EDAX analysis of hot corroded PCGTA welded dissimilar Monel 400 and AISI 304 (Composite Region) employing (a) ER309L (b) ERNiCu-7 and (c) ERNiCrFe-3 filler wires subjected to Na₂SO₄ + V₂O₅ (60%) at 600 °C.

intensities of NiO, FeO and Cr₂O₃ and smaller intensities of Cu₂O, NiCr₂O₄ are formed on the weldments employing ERNiCrFe-3 filler wire.

3.3.4. SEM/EDAX analysis

SEM micrographs of the PCGTAW specimens with three different filler wires showing surface morphology after cyclic hot corrosion for 50 cycles at 600 °C are shown in Figures 10a to 10c. The micrographs of all the corroded weldments clearly indicate the tendency spalling of the scale. The scale formed on the HAZ of Monel 400 of ER309L weldments has tiny splats with non-uniform grains and voids; whereas the scale formed on the weld region is appeared to be fragile and easy to spall in nature. The scale on the HAZ of AISI 304 is found to have large sized splats with voids and needle shaped oxides. In case of ERNiCu-7 weldments, the appearance of oxide scale in HAZ of Monel 400 is found to be spongy with the voids; the weld region and the HAZ of AISI 304 has the needle shaped oxide scale formation which gives an intuit of spalling. The granular, adhesive splats of oxides are observed in the HAZ of Monel 400 of ERNiCrFe-3 weldments; in addition the weld region has tiny, uniform granules of the oxide scales and the HAZ of AISI 304 has the fragile and granular scales.

Point EDAX analysis on the scale formed on the HAZ of Monel 400 of ER309L weldments clearly indicate the formation of NiO, Cr₂O₃, FeO and the spinels of chromium and nickel vanadates; whereas the weld region has higher magnitudes of FeO, Cr₂O₃ and considerable amounts of NiO and the spinels of FeV₂O₄ and CrVO₄, traces of sulphides of Fe and Cr; the HAZ of AISI 304 has been enriched with the Cr₂O₃, FeO and fewer amounts of NiO; in addition to this, the spinels of CrVO₄, NiVO₃ are observed in the HAZ of AISI 304.

For ERNiCu-7 weldments, the weld region has the FeO, Cr₂O₃, the spinels of CrVO₄ and lesser amounts of NiO; whereas the HAZ of Monel 400 has the same content of the above mentioned oxides and spinel with higher content of NiO or the spinel of NiVO₃. Likewise, the HAZ of AISI

304 is enriched with FeO, Cr₂O₃ and the spinels include FeV₂O₄ and CrVO₄. In case of ERNiCrFe-3 weldments, the weld region and the HAZ of Monel 400 have the major constituents of NiO and the spinel of NiVO₃ and considerable amounts of V₂O₅. The presence of Cr₂O₃, Cu₂O and FeO is found be at the least amounts in these zones. However the HAZ of AISI 304 has considerable amounts of FeO, NiO and the spinels of CrVO₄ and FeV₂O₄. Table 4 indicates the hot corrosion data of the bimetallic combinations of Monel 400 and AISI 304.

4. Discussions

Dissimilar joints of AISI 304 and Monel 400 could be obtained from PCGTA welding processes using ER309L, ERNiCu-7 and ERNiCrFe-3 filler materials. The room temperature mechanical properties are good for the joints obtained while employing ERNiCu-7 and ERNiCrFe-3 fillers. The unmixed zone (white layer formation) is found to be in meagre amounts for all the filler wires employed for PCGTA weldments. However the hot cracking tendency is more for ER309L welds which could be witnessed from Figure 3. The presence of Niobium content in ERNiCrFe-3 and Al, Ti additions in ERNiCu-7 may contribute for the better hot cracking resistance as compared to ER309L filler wires. This is in agreement with Sadek et al.²

It is evident that PCGTA welding normally exhibits grain refinement at the weld region. Hence PCGTA welding of dissimilar Monel 400 and AISI 304 resulted in the failure which occurred at the parent metal of AISI 304. It confirms that the weld strength of the PCGTA weldments is higher or equal to the candidate materials employed. The degree of ductility and strength is found to be more for the weldments utilizing ERNiCu-7 and ERNiCrFe-3 which is also evident from the formation of large dimples and micro-voids present in the weldments. Furthermore the fractographs of tensile tested specimen of ER309L weld joints shows the presence of relatively small sized dimples and higher quantities of tearing ridges which shows brittle nature. In addition, the

Table 4. Hot corrosion data of PCGTA welded dissimilar Monel 400 and AISI 304 subjected to Na₂SO₄ + 60% V₂O₅ environment at 600 °C.

	Filler wire	XRD	ZONE	SEM/EDAX
Na ₂ SO ₄ + 60% V ₂ O ₅ Environment PCGTA Welding of Monel 400 and AISI 304	ER309L	NiO and, Cu ₂ O form the major intensities and lesser intensities of Cr ₂ O ₃ and FeO.	HAZ- AISI 304	Cr₂O₃, FeO and fewer amounts of NiO; in addition to this, the spinels of CrVO₄, NiVO₃
			Weld	FeO, Cr₂O₃ and considerable amounts of NiO and the spinels of FeV₂O₄ and CrVO₄, traces of sulphides of Fe and Cr
			HAZ - Monel 400	NiO, Cr₂O₃, FeO and the spinels of chromium and nickel vanadates
	ERNiCu-7	Major intensities of NiO, Cu ₂ O, Ni ₂ CuO ₃ and lower intensities of FeO and Cr ₂ O ₃	HAZ- AISI 304	FeO, Cr₂O₃ and the spinels include FeV₂O₄ and CrVO₄
			Weld	FeO, Cr₂O₃, the spinels of CrVO₄ and lesser amounts of NiO
			HAZ - Monel 400	FeO, Cr₂O₃, the spinels of CrVO₄, NiO or the spinel of NiVO₃
	ERNiCrFe-3	Major intensities of NiO, FeO and Cr ₂ O ₃ and smaller intensities of Cu ₂ O, NiCr ₂ O ₄	HAZ- AISI 304	FeO, NiO and the spinels of CrVO₄ and FeV₂O₄.
			Weld	NiO and the spinel of NiVO₃ and considerable amounts of V₂O₅.
			HAZ - Monel 400	

failure in the fusion boundary of the E309 L weld joint is primarily due to the compositional dilution in the weld metal as reported by Rudovskii et al.⁹ It is further confirmed that the segregation/secondary phase formation in the weld interface reduces the tensile strength which is evident from the microstructure.

From the corrosion results, it is evident that the parent metal Monel 400 has better corrosion resistance as compared to the parent metal of AISI 304 and other zones of the PCGTA weldments employing different filler wires. As the parent metal of Monel 400 has higher amounts of Ni and Cu, the formation of NiO and the refractory spinel oxide NiVO₃ afford the protective scale which prevents the base metal from the corrosion attack due to Na₂SO₄ + 60% V₂O₅ environment (Figure 10). It is well matching with the findings of Sidhu et al.¹⁷ They reported that the hot corrosion resistance of the Superni-75 has been attributed to the formation of uniform, homogeneous and adherent thick layer of the scale consisting mainly of oxides of nickel and chromium, and to the presence of refractory nickel vanadate.

It is clear from thermogravimetric analysis of PCGTA weldments that the weight gain is observed in the weld region of ER309L weldments (Figure 8). The scales formed on ER309L Weld, HAZ (AISI 304 side) were fragile and the scale indicated tendency to crack (Figure 10). In the case of other zones of the weldment, surfaces of the scale become uneven and pits were observed at places from where spalling had taken place. SEM/EDAX analysis conveyed the formation of lesser amounts of NiVO₃ in both the regions. In case of ERNiCu-7 weldments, all the zones had shown the less weight changes. Even though small superficial cracks were observed on the scale of ERNiCu-7 weld specimens after 50 cycles, the scale was continuous and more adhesive (Figure 10) as compared to ER309L weldments. The presence of additions such as Al and Ti would provide better corrosion resistance of the weld region of ERNiCu-7 weldments. Jayaganthan et al.¹⁸ conducted hot corrosion studies on Ni and Fe-based superalloys in an aggressive environment containing Na₂SO₄. 60% V₂O₅ at 900 °C. They reported that NaVO₃ acts as a catalyst and also serves as an oxygen carrier to the base alloy through the open pores present on the surface, which will lead to the rapid corrosion. Also, the spinel oxide NiAl₂O₄ formed during the hot corrosion showed better corrosion resistance as compared to NiO. Even though the corrosion resistance of ERNiCu-7 weld was found to be poor in Na₂SO₄ + 60% V₂O₅ environment, it is superior as compared to ER309L weld and weld interface. It was inferred that the formation of the secondary phase γ₁ in Ni-Cu-Cr systems, which was Cr-rich and had the same FCC crystallographic structure as the Ni rich phase γ₂. Therefore, the dilution of Cr in the Ni-Cu weld metal could cause the formation of the Cr-rich secondary phase, which could affect the corrosion properties. In case of ERNiCrFe-3 weldments, the HAZ of AISI 304 has undergone severe attack due to the molten salt environment. This may be due to the formation of the spinel FeV₂O₄ and CrVO₄ which contributed for the corrosion attack. It was reported that the effect of adding Cr to Ni was found to be beneficial in the Na₂SO₄ melt. However, on increasing the VO₃⁻ concentration in the melt, this effect has diminished, becoming harmful in pure NaVO₃ due to the formation of the non-protective CrVO₄¹⁹.

It is evident from the results that the hot corrosion on the molten salt environment did not follow the parabolic rate.

This could be attributed to the formation and spallation of oxide scales from the various coupons. Weight gain was observed in almost all the coupons however the trend was oscillatory in nature. This is supported by other researchers that the deviation in the parabolic rates was attributed to the cyclic scale growth.

Also the condensed vanadates of sodium are highly corrosive and can markedly increase the rate of oxidation of nickel base alloys²⁰. Presence of refractory nickel vanadate Ni(VO₃)₂ acts as diffusion barrier of oxidizing species which prevents the corrosion attack²¹. The presence of sulphur in the form of sulphates has been reported to cause internal sulphidation of the alloy beneath the external oxide layer. From the extensive literature review, it is found that the weldments subjected to molten salt environment normally follow the parabolic rate law. During the initial stages of corrosion, the molten salt gets into the pores of the component leading to accelerated attack followed by the steady state behavior after few cycles. From the parabolic rate law, it is possible to determine the kinetics of corrosion and the mode of corrosion.

In general, the PCGTA weldments showed lower resistance to corrosion attack due to the grain refinement (Figure 3). On comparing the weld regions of various filler wires, ERNiCrFe-3 weldment has shown the better corrosion resistance as compared to ER309L and ERNiCu-7 weldments (Figure 8). From the SEM/EDAX analysis, it is clear that the weld region employing ERNiCrFe-3 filler wire is enriched with NiVO₃ (Figure 10). This refractory spinel strengthens the subsurface by preventing further corrosion attack. From the results obtained from all the analysis, the HAZ of AISI 304 for all the filler wires has also undergone the corrosion attack. It is well understood from the SEM/EDAX analysis that the non-protective CrVO₄ and FeV₂O₄ scales are formed and contributed for the corrosion.

As a nutshell, this study reported that the bimetallic combinations of Monel 400 and AISI 304 could be welded successfully employing ERNiCu-7 and ERNiCrFe-3 by PCGTA welding process. As far as the mechanical properties are concerned, both these filler metals exhibited better strength. However the ERNiCrFe-3 weldments offered better corrosion resistance compared to ERNiCu-7 weldments. Based on the outcomes of the study, it is recommended to employ ERNiCrFe-3 for welding Monel 400 and AISI 304 by PCGTA welding to accrue beneficial results.

5. Conclusions

The conclusions from the present study involving dissimilar weldment of Monel 400 and AISI 304 by two types of welding process namely Pulsed Current Gas Tungsten Arc Welding (PCGTAW) employing three filler metals such as ER309L, ERNiCu-7 and ERNiCrFe-3 are outlined as follows:

- Sound welds of Monel 400 and AISI 304 were obtained by PCGTA welding process for all three filler wires.
- Macrostructure examination revealed that the macroscale deficiencies were found to be absent for all the weldments
- Weldments obtained by the filler materials such as ERNiCu-7 and ERNiCrFe-3 by both the welding process exhibit satisfactory mechanical properties as compared to ER309L.

- Hot cracking tendency was observed in ER309L weldments. It is due to the fact that the dilution of Ni based alloy by a dissimilar metal can be tolerated to certain extent. When the filler wire of ER309L is used to weld Monel 400 and AISI 304, any significant amount of copper pick up from Monel 400 would cause the weld metal to induce hot cracking tendency.
- Segregation was found to be almost absent for the PCGTA weldments which could be due to current pulsing.
- The higher hardness in the weld interface in case of PCGTA weldments contributed for the maximum tensile strength. On conducting the tensile studies of PCGTA weldments employing ERNiCu-7 and ERNiCrFe-3 filler metals, the fracture occurred at the parent metal of AISI 304 on all the three trials. This clearly indicates that the strength of these welds are higher as compared to the strength of the base metals employed in the study.
- The sequence for the tensile strength of PCGTA welded dissimilar Monel 400 and AISI 304 could be arranged as follows: $W_{\text{ERNiCu-7}} \cong W_{\text{ERNiCrFe-3}} > W_{\text{ER309L}}$; PCGTA Weldments employing ERNiCu-7 and ERNiCrFe-3 filler wires offer almost the same tensile strength.
- Molten salt environment prevailing in the power plant ($\text{Na}_2\text{SO}_4 + 60\% \text{V}_2\text{O}_5$) – the performance of PCGTA welded dissimilar Monel 400 and AISI 304 can be arranged in the order as follows: $W_{\text{ERNiCrFe-3}} > W_{\text{ERNiCu-7}} > W_{\text{309L}}$.
- The non- protective CrVO_4 and FeV_2O_4 scales contributed for the molten salt corrosion attack. The presence of refractory nickel vanadate $\text{Ni}(\text{VO}_3)_2$ acts as diffusion barrier of oxidizing species which prevents the corrosion attack in the ERNiCrFe-3 welds.
- The oscillatory trend of hot corrosion could be due to the cyclic scale growth and spallation of protective oxide scales.

References

1. Mohandas T, Satyanarayana VV and Madhusudhan Reddy G. Dissimilar metal friction welding of austenitic-ferritic stainless steels. *Journal of Materials Processing Technology*. 2005; 160(2):128-137.
2. Sadek AA, Abass M, Zaghoul B, Elrefaey A and Ushio M. Investigation of dissimilar Joints between Low Carbon steel and Monel 400. *Transactions of JWRI*. 2000; 29(1):21-28.
3. Janaki Ram GD, Venugopal Reddy A, Prasad Rao K, Madhusudhan Reddy G and Sambasiva Rao A. Effect of magnetic arc oscillation on microstructure and properties of Inconel 718 GTA welds. *Transactions of The Indian Institute of Metals*. 2006; 59(1):85-97.
4. Madhusudhan Reddy G, Gokhale AA and Prasad Rao K. Weld microstructure refinement in a 1441 grade aluminium-lithium alloy. *Journal of Material Science*. 1997; 32(15):4117-4126.
5. Madhusudhan Reddy G, Gokhale AA and Prasad Rao K. Optimization of pulse frequency in pulse current gas tungsten arc welding of Al-Lithium alloy steels. *Journal of Material Science and Technology*. 1998; 14(1):61-66.
6. Grill A. Effect of arc oscillations on the temperature distribution and microstructure in GTA tantalum welds. *Metallurgical and Materials Transactions B*. 1981; 12(4):667-674. <http://dx.doi.org/10.1007/BF02654135>
7. Vijay Ukadgaonker G, Sunil Bhat, Jha M and Deasai PB. Fatigue crack growth towards the weld interface of alloy and maraging steels. *International Journal of Fatigue*. 2008; 30(4):689-705. <http://dx.doi.org/10.1016/j.ijfatigue.2007.05.005>
8. Oates WR and Saitta AM. *Welding handbook: materials and applications*. Miami: American Welding Society; 1998. p. 59.
9. Rudovskii YA, Leleko LN and Timofeeva EY. Method for welding Monel metal to a corrosion-resisting steel. *Welding Production*. 1984; 31(7):44-45.
10. Paul AR, Naik MC and Kaimal KNG. Mass transport of Chromium and Nickel in Monel-400. *Journal of Nuclear Materials*. 1975; 58(2):205-210. [http://dx.doi.org/10.1016/0022-3115\(75\)90108-7](http://dx.doi.org/10.1016/0022-3115(75)90108-7)
11. Salehi Yegaie Y, Kermanpur A and Shamanian M. Numerical simulation and experimental investigation of temperature and residual stresses in GTAW with a heat sink process of Monel 400 plates. *Journal of Materials Processing Technology*. 2010; 210(13):1690-1701.
12. Shams El Din AM, El Dahshan ME and Taj El Din AM. Dissolution of copper and copper-nickel alloys in aerated dilute HCl solutions. *Desalination*. 2000; 130(1):89-97.
13. Kim YH, Frankel GS, Lippold JC and Guaytima G. Development of a chromium-free consumable for austenitic stainless steels. Part 1: monel (Alloy 400) filler metal. *Corrosion*. 2006; 62(1):44-53. <http://dx.doi.org/10.5006/1.3278251>
14. Liang D, Sowards JW, Frankel G S, Alexandrov BT and Lippold JC. A corrosion study of nickel-copper and nickel-copper-palladium welding filler metals. *Materials and Corrosion*. 2010; 61(11):909-919. <http://dx.doi.org/10.1002/maco.200905583>
15. Otero E, Pardo A, Hernandez J and Perez, FJ. The hot corrosion of IN-657 superalloy in $\text{Na}_2\text{SO}_4\text{-V}_2\text{O}_5$ melt eutectic. *Corrosion Science*. 1990; 32(7):677-83.
16. Devendranath Ramkumar K, Arivazhagan N and Narayanan S (2012). Effect of filler materials on the performance of Gas Tungsten arc welded AISI 304 and Monel 400. *Materials & Design*. 40:70-79.
17. Sidhu TS, Prakash S and Agarwal RD. Study of molten salt corrosion of superni-75 using thermogravimetric technique. *Journal of Naval Architecture and Marine Engineering*. 2006;3:77-82.
18. Mahesh RA, Jayaganthan R and Prakash S. A study on hot corrosion behaviour of Ni-5Al coatings on Ni-and Fe-based super alloys in an aggressive environment at 900 °C. *Journal of Alloys and Compounds*. 2008; 460(1-2):220-231.
19. Xu H, Hocking MG and Sidky PS. Sulfidation-oxidation behavior of alloy 800H in SO₂-O₂ and H₂-H₂S-CO-CO₂ atmospheres. *Oxidation of Metals*. 1994; 41(1-2):81-101.
20. Lambert P, Champagne B and Arseneault B. Oxidation and Hot Corrosion in Na₂SO₄-10%V₂O₅ of Ni-17Cr-6Al-0.5Y and Ni-16Cr-5.7Al-0.47Y-5Si MCrAlY Alloys at 700 °C. *Canadian Metallurgical Quarterly*. 1991; 30(2):125-130. <http://dx.doi.org/10.1179/cmqr.1991.30.2.125>
21. Gitanjali. *Role of inhibitors on hot corrosion of superalloys in Na₂SO₄-V₂O₅ environment* [Thesis]. Roorkee: Indian Institute of Technology; 2003.